JOURNAL OF SYNCHROTRON RADIATION
ISSN 1600-5775

An efficient plane-grating monochromator based on conical diffraction for continuous tuning in the entire soft X-ray range including tender X-rays (2–8 keV)

Werner Jark*

X-ray Fluorescence Beamline, Elettra – Sincrotrone Trieste ScpA, SS 14, km 163.5 in Area Science Park, Basovizza, 34149 Trieste, Italy. *Correspondence e-mail: werner.jark@elettra.eu

Received 3 September 2015
Accepted 16 November 2015

Edited by P. A. Pianetta, SLAC National Accelerator Laboratory, USA

Keywords: grating monochromator; plane grating; X-rays; conical diffraction; spectral resolution.

Recently it was verified that the diffraction efficiency of reflection gratings with rectangular profile, when illuminated at grazing angles of incidence with the beam trajectory along the grooves and not perpendicular to them, remains very high for tender X-rays of several keV photon energy. This very efficient operation of a reflection grating in the extreme off-plane orientation, *i.e.* in conical diffraction, offers the possibility of designing a conical diffraction monochromator scheme that provides efficient continuous photon energy tuning over rather large tuning ranges. For example, the tuning could cover photon energies from below 1000 eV up to 8 keV. The expected transmission of the entire instrument is high as all components are always operated below the critical angle for total reflection. In the simplest version of the instrument a plane grating is preceded by a plane mirror rotating simultaneously with it. The photon energy selection will then be made using the combination of a focusing mirror and exit slit. As is common for grating monochromators for soft X-ray radiation, the minimum spectral bandwidth is source-size-limited, while the bandwidth can be adjusted freely to any larger value. As far as tender X-rays (2–8 keV) are concerned, the minimum bandwidth is at least one and up to two orders of magnitude larger than the bandwidth provided by Si(111) double-crystal monochromators in a collimated beam. Therefore the instrument will provide more flux, which can even be increased at the expense of a bandwidth increase. On the other hand, for softer X-rays with photon energies below 1 keV, competitive relative spectral resolving powers of the order of 10000 are possible.

1. Introduction

The advantage of the extreme off-plane orientation of reflection gratings over the classical orientation for high-efficiency diffraction was pointed out some time ago by Greig & Ferguson (1950). In the classical grating orientation the trajectory of the incident beam is perpendicular to the grating ruling, as shown on the left in Fig. 1 for a rectangular or laminar grating profile. As far as soft X-rays with photon energies E between 0.28 keV and 8 keV are concerned, their monochromatization will require the use of grazing incidence (see, for example, Werner, 1977), as all optics in a related beam transport system, including the grating, need to be operated below the cut-off angle for total external reflection (Compton, 1923). For this condition part of the incident intensity will be lost in the ruled structure due to shadowing effects. Shadowing effects can be avoided in the extreme off-plane orientation (see, for example, Jark & Eichert, 2015, 2016) when the beam trajectory is parallel to the grooves, as shown on the right in Fig. 1. This will then result in a larger

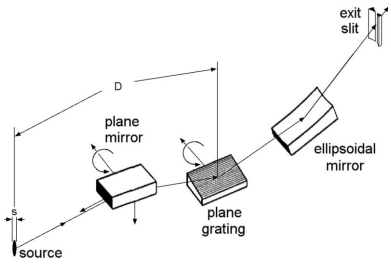

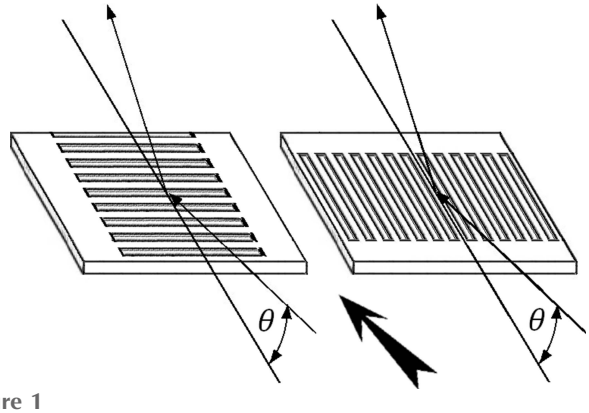

Figure 1
Beam trajectories at grazing incidence in laminar gratings, oriented for vertical beam deflection in the classical orientation on the left and in the extreme off-plane orientation on the right. In the latter case the beam trajectory is parallel to the grooves.

efficiency. Originally the off-plane orientation was proposed by Greig & Ferguson (1950) for a grating with sawtooth-shaped grooves, arranged to form a staircase with rather small slope, as shown in Fig. 2, and it was successfully tested by them using long-wavelength infrared radiation. Such a grating is operated very favourably in the so-called blaze-maximum configuration, or simply 'in blaze', when the desired diffraction order is simply specularly reflected on top of the stairs, which thus act like small mirrors as shown in Fig. 2. A grating operated in blaze in the extreme off-plane orientation will then provide the highest relative diffraction efficiency. It has already been experimentally verified by Werner (1977) that the diffraction efficiency in the latter off-plane orientation can be significantly superior to the efficiency in the classical orientation for soft X-rays with photon energies up to E = 1.5 keV. In principle, this encouraging result should have allowed for the construction of efficient soft X-ray monochromators for synchrotron radiation, as proposed by Werner & Visser (1981). It is thus surprising that only a few such realisations have been reported, for example by Frassetto *et al.*

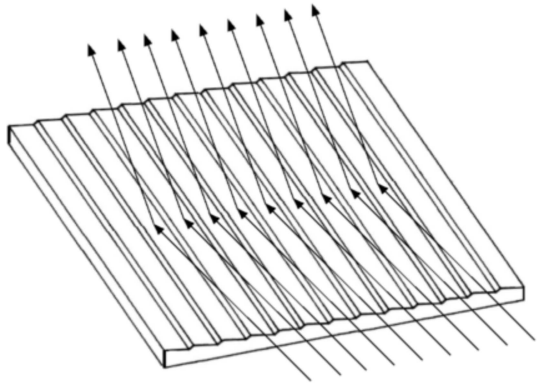

Figure 2
Beam trajectories at grazing incidence in sawtooth profile gratings, when the grating is operated in the extreme off-plane orientation and in blaze-maximum, *i.e.* when the rays for a desired diffraction order are simply specularly reflected at the grooves. Then the incident and the exiting diffracted rays are found in the plane of incidence of the single groove and parallel to the grooves.

(2011), for use at lower photon energies in the extreme ultraviolet (EUV) range. This can be understood because, at very grazing angles of incidence, according to Werner & Visser (1981) and Cash (1982), the dispersion in a grating in the classical orientation provides a significantly smaller bandwidth than the dispersion in conical diffraction. In the design of soft X-ray monochromators for synchrotron radiation, the achievement of the smallest possible spectral bandwidth was almost always given priority over the supply of maximum possible photon flux (see, for example, Chen & Sette, 1989). The situation is the opposite for space astronomy, where priority needs to be given to the highest possible transmission/efficiency in an instrument with minimum number of components. In this case spectral analysis is the goal, which requires the use of a spectrometer in which moving parts can be avoided. It is thus proposed to use for this purpose reflection gratings in the extreme off-plane orientation in the simplest possible setup, *i.e.* in the convergent beam behind a focusing mirror (*e.g.* Cash, 1982, 1983; McEntaffer *et al.*, 2004, 2013). This spectrometer is proposed as a two-optical-component system, and its use is restricted to lower-energy soft X-rays in the 0.2–1 keV range. Such a simple configuration cannot be employed when a synchrotron radiation beam is to be monochromated in a fixed slit and with fixed direction for the exiting beam. On the other hand, the required rather complex optical structure in the proposed beam transport system of Werner & Visser (1981) for an on-blaze conical diffraction monochromator presented another obstacle to its realisation.

It was verified by Jark & Eichert (2015, 2016), for a laminar grating with a groove density of 1220 lines mm^{-1}, that high diffraction efficiencies can also be obtained from reflection gratings in the off-plane mount for tender X-rays with photon energies above 4 keV. The total diffracted intensity from the grating was found to be identical to the total reflected intensity from a mirror with the same coating. About 30% of the diffracted intensity was directed into each of the two first-order diffraction peaks. This is to be compared with an expected maximum relative efficiency in a laminar grating profile of 40%. This latter limit is due to the fact that the diffraction at a laminar grating profile in the extreme off-plane orientation is symmetric and thus another 40% is diffracted into a symmetric order. The observed absolute efficiencies for diffraction into each first order were 15.5% for 4 keV photon energy and 12.5% for 6 keV photon energy. Though relatively small, these efficiencies nevertheless compare favourably with at least twofold smaller efficiencies of 7.2% and 5% from a blazed grating (blaze angle 0.4°) with more favourable smaller groove density of 600 lines mm^{-1}, when operated in the classical orientation at the same photon energies (Cocco *et al.*, 2007). The intensity loss due to the symmetric intensity splitting in a laminar grating profile will not be observed in a blazed grating, which can provide better directional selectivity. Werner (1977) has already observed a higher relative efficiency of almost 60%, though for a lower photon energy of 1.5 keV. It is expected that state-of-the-art blazed gratings should thus also provide higher relative efficiencies at larger photon energies (>1.5 keV). With this expectation one should

be able to use only one single grating, *i.e.* a plane grating in the off-plane mount, for the beam monochromatization over the entire soft X-ray range with photon energies between 0.28 keV and 8 keV. As is usual when diffraction gratings are employed, such an optical system will permit the spectral bandwidth to be freely adjusted above a certain lower limit. This feature has not been described yet for other tender X-ray and hard X-ray ($E > 8$ keV) monochromators, which are based on diffraction crystals. Instead it can also be provided by refraction, as was applied in a mosaic prism lens monochromator by Liu *et al.* (2012). Liu *et al.* (2012) showed the feasibility for bandwidth variation up to a relative resolving power of $E/\Delta E = 50$, while Jark (2012, 2013) presented a convenient tuning scheme with a fixed exit slit and discussed the limitations for the achievable bandwidth. The latter is found to be of the order of $E/\Delta E = 200$, limited by diffraction. However, as the mosaic prism lens monochromator is based on transmission, the unavoidable absorption in matter makes refractive optics rather inefficient for tender X-rays. Consequently this study will discuss in detail the operation parameters for a soft X-ray grating monochromator, which can also cover the tender X-ray range by utilizing a reflection grating in the off-plane mount. It will be investigated in particular whether or not the optical concept in the originally proposed on-blaze conical diffraction monochromator can be simplified to a more convenient operation scheme.

2. Schemes for conical diffraction monochromators for the X-ray range

2.1. Originally proposed concept and simplifications

The proposed optical scheme of Werner & Visser (1981) for an on-blaze conical diffraction monochromator is shown in Fig. 3. This monochromator was optimized to a rather symmetric optical concept. The beam passing the entrance slit is collimated upstream of the grating horizontally and vertically by a paraboloidal mirror. This beam collimation will minimize the possible aberrations in the beam, which the diffraction process could introduce. For photon energy tuning, the angles of grazing incidence and grazing exit onto the grating are varied, such that the grating stays in the blaze-maximum condition. This is achieved by simply translating the properly inclined grating vertically and by rotating two plane mirrors next to it simultaneously in opposite directions. Then neither the position nor the direction of the in-blaze diffracted beam exiting from the second mirror will change during tuning. The photon energy selection is achieved by focusing this latter beam direction by use of a stationary paraboloidal mirror into a stationary exit slit. In this scheme the photon energy will increase when the angles of grazing incidence onto the moving components decrease, *i.e.* when the grating is raised as shown in Fig. 3. Werner & Visser (1981) preferred this driving scheme for its simplicity over the combination of a grating with a single plane mirror. However, it is inconvenient that the angle of grazing incidence onto the grating increases twofold with respect to the increase in the corresponding angle of grazing incidence onto the plane mirrors. This can be avoided when only a single plane mirror is involved. In fact, as applied already by Greig & Ferguson (1950), the blaze-maximum condition can be maintained during tuning in a stationary exit direction by rotating only one plane mirror simultaneously with the grating. In order to keep the position of the exiting beam stationary one will additionally have to translate at least one of the components such that the beam displacement in the plane of incidence of the plane mirror, *i.e.* the plane containing the incident beam and the normal to the surface, remains constant. Note that most of the driving schemes for double-crystal monochromators were developed for exactly this purpose (see, for example, Matsushita, 1983).

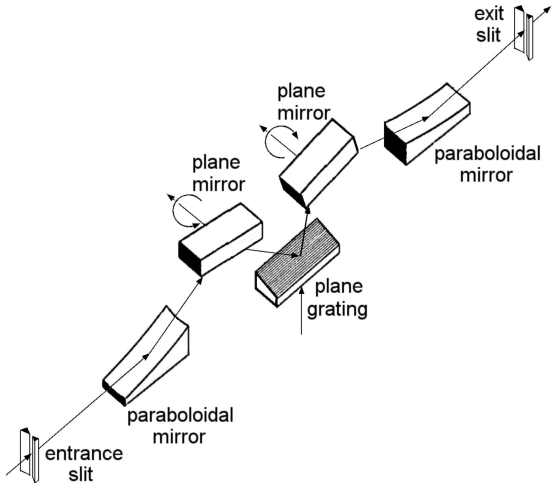

Figure 3
Optical scheme of the originally proposed on-blaze conical diffraction monochromator (Werner & Visser, 1981). The beam trajectory is shown for a single ray progressing from the left to the right. The indicated grating translation and mirror rotations will provide increasing photon energy during tuning.

2.2. Simpler variants

It has also already been proposed by Koike & Namioka (2004) and by Frassetto *et al.* (2011) to remove both plane mirrors. Then tuning is achieved by rotating only the grating around an axis that lies in its surface and is parallel to the grooves. In this case the blaze-maximum condition is achieved for only one particular photon energy and the efficient tuning is limited to roughly a factor of two to three in photon energy. Koike & Namioka (2004) proposed such an instrument for tuning in photon energy between 1 keV and 4 keV; however, no related realisation and experimental performance data are reported.

2.3. Present proposal

Here the goal is on-blaze tuning over larger tuning ranges. This will require at least a plane-mirror/plane-grating pair in combination with a stationary focusing mirror and a stationary exit slit. The final question is thus whether the collimation of the incident beam can be avoided by either accepting the residual aberrations in the beam or removing them by other

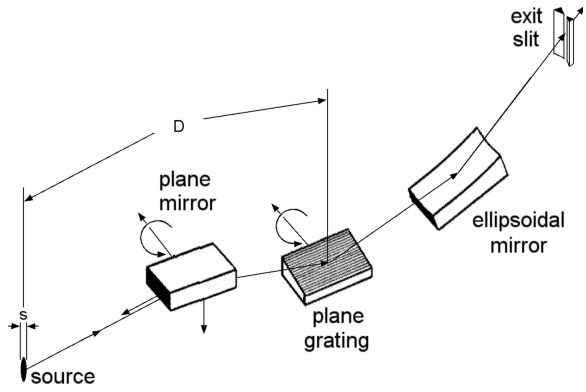

Figure 4
Simplified conical diffraction monochromator without any incident beam collimation and with simultaneously rotating plane mirror and plane grating. The translations and rotations along and around the indicated axes will lead to increasing photon energy. The grating surface is inclined with respect to the surface of the plane mirror. The source size in the direction of its smaller dimension is denoted s, and the distance of the grating from it is D.

means. Then the optical system could be simplified to the scheme shown in Fig. 4, in which an ellipsoidal mirror will provide the required focusing. Related driving and mounting schemes have already been discussed in several monochromator schemes (see, for example, Kunz *et al.*, 1968; Dietrich & Kunz, 1972; Cerino *et al.*, 1980; Hunter *et al.*, 1982; Matsushita, 1983; Jark & Kunz, 1986).

3. Theoretical considerations

3.1. Conical diffraction

According to Werner (1977) and as shown in Fig. 5, when an X-ray beam impinges on a reflection grating in the off-plane orientation, such that the angle between the beam and the grooves is γ, then all intensity regardless of the wavelength and of the diffraction order number m is diffracted through an arc, which forms a cone as shown in Fig. 5. The axis of this cone is parallel to the grooves and its half-opening angle is identical to the beam inclination angle γ. This angle will not vary as long as the incident beam moves on a cone with the same angle and the same axis. This situation is described as conical diffraction and the related grating equation is most conveniently written in spherical coordinates as (Werner, 1977)

$$\sin\gamma(\sin\alpha + \sin\beta_m) = m\lambda/p. \tag{1}$$

Here p is the periodicity of the grating, and the azimuthal position angles for the source and for the diffracted orders of a given wavelength λ on the cones are denoted α and β_m, respectively. The blaze-maximum condition is fulfilled when the blaze angle of the grating, *i.e.* the inclination angle of the reflecting part of the grooves with respect to the grating surface, coincides with the position angle α for the source, and when $\beta_m = \alpha$. For the monochromator operation, $\beta_1 = \alpha$ will be considered. Then α may be varied, and it will thus not always be identical to the blaze angle of the grating.

For further considerations it is more convenient to use a rectangular coordinate system, following Cash (1982). As shown on the right in Fig. 5, such a system relates the diffraction to the angle of grazing incidence θ, which is the variable in the monochromator. The vertical reference plane contains the centre axis of the cones and it is perpendicular to the grating surface. The angle ψ is then the orientation angle of the trajectory of the incident beam with respect to this latter vertical reference plane. Both angles θ and ψ will be assumed to be rather small and one can thus use

$$\gamma = \left(\psi^2 + \theta^2\right)^{1/2}. \tag{2}$$

For a given wavelength one will then find the diffraction peaks at the rectangular coordinates

$$\varphi_m = m(\lambda/p) - \psi \tag{3}$$

and

$$\vartheta_m = \left[\theta^2 + 2m(\lambda/p)\psi - (m\lambda/p)^2\right]^{1/2}. \tag{4}$$

It is interesting at this point to recognize that the diffraction angle φ_m does not depend on the angle θ, which is measured orthogonal to it.

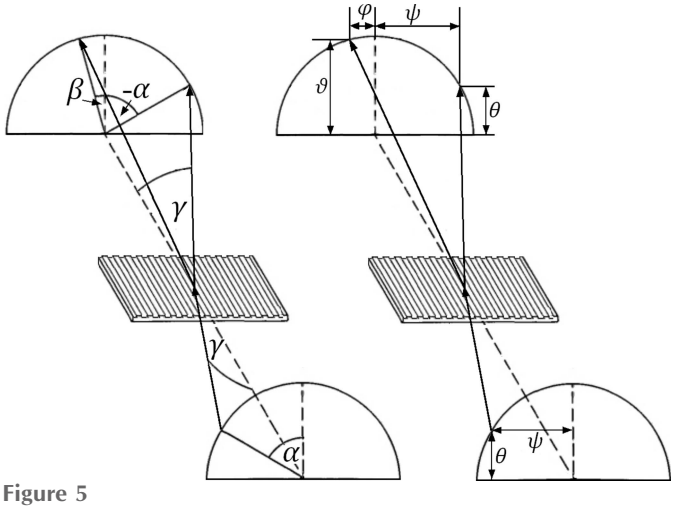

Figure 5
Orientation of a laminar grating profile for incident beams close to the extreme off-plane orientation and for vertical beam deflection. The commonly used angular convention for conical diffraction is shown on the left, while on the right a rectangular coordinate system is used.

3.2. Spectral resolving power

The important reference parameter is the source-size-limited spectral bandwidth. It is obtained from equation (3) for operation of the grating in the first diffraction order $m = 1$ as

$$\Delta\lambda = \frac{\partial}{\partial\psi}\lambda\Delta\psi = p\Delta\psi. \tag{5}$$

Here $\Delta\psi$ is the residual angular spread in the incident beam due to the finite source size. This angular spread, which is the ratio s/D between the source size s and its distance from the grating D, does not change upon diffraction and thus deter-

mines the required setting of the exit slit, which depends linearly on the focal length of the chosen mirror. Equation (5) then indicates that the spectral bandwidth to be provided in this condition in conical diffraction from a grating is constant. This is rather unusual for soft X-ray monochromators. Consequently, for comparison purposes, the relative spectral resolving power will be calculated as

$$\frac{\lambda}{\Delta\lambda} = \frac{E}{\Delta E} = \frac{\lambda D}{ps}. \quad (6)$$

3.3. Effect of slope errors

When the optical components are not perfectly shaped, then any remaining wavyness in the surface will add an angular spread to the reflected/diffracted beams, which can eventually lead to an increase in the spot size in the focus beyond the size of the focused source. An excessive increase will then reduce the achievable spectral bandwidth. As introduced by Takacs *et al.* (1987) for X-ray optics the mirror shape perfection is commonly expressed as the r.m.s. slope error $\sigma_{\rm rms}$. Such a slope error will superimpose an angular spread into the reflected beam given by $\eta_{\rm FWHM,tan} = 2(2\sqrt{2\ln 2})\sigma_{\rm rms}$ for the case of tangential reflection, *i.e.* in the plane of incidence of an optical component.

In the orthogonal direction, *e.g.* applying focusing orthogonal to the plane of incidence, the added angular spread is given by $\eta_{\rm FWHM,sag} = 2(2\sqrt{2\ln 2})\sigma_{\rm rms}\sin\theta$. Compared with the equation for the tangential case, the latter equation contains additionally the geometrical factor $\sin\theta$, which is here $\ll 1$. The latter factor is always rather small for soft X-rays and it thus received the name 'forgiveness' factor. The presented optical scheme, as shown in Fig. 4, has the advantage that the additional angular spread in the direction of the dispersion by the grating is introduced by the surface imperfections in the sagittal direction by all components. Then the 'forgiveness' factor will make any effect on the spectral resolution, caused by rather small slope errors in state-of-the-art X-ray optics, negligible in the presented configuration.

4. Discussion of expected performance

4.1. Boundary conditions for the monochromator operation

For reference purposes two different beamlines will be considered. The first is a bending-magnet beamline at Elettra, *i.e.* the X-ray fluorescence beamline described by Jark *et al.* (2014), where the first optics can be operated at a distance D = 12 m from a source with full width at half-maximum (FWHM) size s_z = 66 µm in the vertical direction and s_x = 330 µm in the horizontal direction. These numbers are characteristic for bending-magnet sources at lower-energy storage rings. Alternatively an odd-numbered ESRF undulator beamline (ESRF, 2015) is considered with threefold-larger source distance D = 36 m and with s_z = 20 µm and s_x = 140 µm. These latter values are now more characteristic for the beam properties at insertion devices at new-generation state-of-the-art synchrotron radiation sources at higher-energy storage rings. For the grating two different groove spacings of p = 820 nm (line density = 1220 lines mm^{-1}) and p = 278 nm (3600 lines mm^{-1}), as used by Jark & Eichert (2015, 2016) and by Werner (1977), are taken. The reference photon energies are chosen as 6 keV (λ = 0.207 nm) and 600 eV (λ = 2.07 nm). The related limiting angles for the operation of Ni coatings in total reflection are θ = 0.57° (0.01 rad) and θ = 4° (0.07 rad) (CXRO, 2015), respectively. The related azimuthal orientation angles for the grating with a line density of 1220 lines mm^{-1} need then to be α = 1.44° for 6 keV photon energy and α = 2.06° for 600 eV. For the grating with 3600 lines mm^{-1} the respective angles need to be about threefold larger. Obviously the blaze angle at the grating cannot be varied between the two indicated values. However, the grating drive could provide related provisions for changing the grating orientation angle α accordingly. Consequently a 1220 lines mm^{-1} grating with constant intermediate blaze angle of about 1.75° will then be operated still close to blaze-maximum.

For the further discussion the grating profile will not be considered explicitly, as only the groove spacing is the relevant parameter. As far as the initially mentioned laminar profile is concerned, this profile will also show a 'blazing' effect for the incident radiation. The diffraction efficiency is maximal when the intensity diffracted in the grooves constructively interferes with the intensity diffracted at the tops. This requires an optical path difference for the longer trajectory through the grooves of an integer multiple of the wavelength (Born & Wolf, 1980). Then the required groove depth d is related to the grating inclination angle α *via* $d = \alpha p/2$. Compared with the blazed profile this grating can also provide maximum efficiency in a photon energy scan with constant inclination angle α; however, the efficiency is expected to be about twofold smaller. Even though the efficiency is reduced by use of this profile, comparison of the available experimental data of Jark *et al.* (2015) with those of Cocco *et al.* (2007), mentioned earlier, indicates that the efficiency of the laminar profile in conical diffraction will significantly exceed the efficiency that could be achieved in the classical orientation even with blazed gratings. In the present condition the laminar profile will provide significant capabilities for higher-order suppression, *i.e.* for the elimination of X-rays with integer multiples of the fundamental photon energy. In fact, in a laminar structure with tops and grooves of equal width, all even orders are theoretically suppressed (Born & Wolf, 1980; Schnopper *et al.*, 1977).

Note that now, for featureless tuning in the vicinity of the Ni L-absorption edges between 850 eV and 1000 eV photon energy (CXRO, 2015), one will have to employ a different coating at the grating. The gratings are to be used behind a square entrance aperture $A_x \times A_z$ with side length $A_x = A_z$ = 4 mm. The maximum beam footprint length $L' = A_{x,z}/\theta$ at the grating thus measures 400 mm for 6 keV photon energy and reduces to 58 mm at 600 eV. It is assumed that the grating is downstream of the plane mirror as shown in Fig. 4. Then the footprint at the plane mirror is rectangular, whereas it is of trapezium shape at the grating due to the inclination of its

Table 1
Spectral resolving power $\lambda/\Delta\lambda$ according to equation (6) for two different photon energies at two different synchrotron radiation sources and for two different groove densities..

	Elettra		ESRF	
	E = 6 keV	E = 600 eV	E = 6 keV	E = 600 eV
For p = 820 nm	50	500	500	5000
For p = 278 nm	150	1500	1500	15000

surface with respect to the surface of the plane mirror. This change of shape will be ignored for the following considerations. The number of illuminated lines, which give the diffraction-limited resolving power, when the monochromator is operated in first order (m = 1) (Born & Wolf, 1980) is then 4880 and 14400 for line densities of 1220 lines mm^{-1} and 3600 lines mm^{-1}, respectively.

4.2. Expected spectral resolving power in comparison with state-of-the-art monochromators

Table 1 reports the ideal achievable resolving powers according to equation (6) for the indicated conditions and taking into account the favourable smaller source dimension s_z. At synchrotron radiation sources this smaller source dimension is always found in the vertical direction. This will then require the incident beam to be deflected horizontally at the grating as well as at the plane mirror, *i.e.* to operate the optics in a horizontal deflection scheme. This is rather uncommon in soft X-ray monochromators for synchrotron radiation. From the data in Table 1 one finds that the resolving powers are almost always limited by the source size; and the diffraction limit, *i.e.* the number of illuminated lines, becomes the limiting factor for photon energies below the discussed lower limit of 600 eV.

At this point the results need to be compared with the standard performance of other monochromator systems for the respective tuning ranges. In the tender X-ray range for photon energies $E > 2$ keV the standard Si(111) double-crystal monochromator provides a constant resolving power of $\lambda/\Delta\lambda$ = 7000 in a collimated beam (Matsushita, 1983). A similar resolving power is also projected to be obtained in the same range by use of a blazed grating in the classical orientation (Cocco *et al.*, 2007). At lower photon energies with $E <$ 1 keV the standard performance for grating monochromators is slightly better with $\lambda/\Delta\lambda \simeq 10000$ (Chen & Sette, 1989). Multilayer monochromators with artificially produced large periodicity coatings instead provide resolving powers of the order of $\lambda/\Delta\lambda$ = 100 (Underwood & Barbee, 1981), which is very similar to the capabilities of the mosaic prism lens monochromator (Liu *et al.*, 2012; Jark, 2013).

From comparison of the data for the present monochromator concept in Table 1 and the presented references one finds that, as far as the operation in the tender X-ray range at Elettra bending magnets is concerned, conical diffraction could provide resolving powers characteristic of multilayer mirrors with the related gain in flux comparable with a double-crystal monochromator. On the other hand, at ESRF undulators the instrument can perform better than multilayer mirrors. This will then permit about an order of magnitude in flux to be gained compared with double-crystal monochromators and more when the exit slit is opened. At the same source, for softer X-rays ($E < 1$ keV), with resolving powers of the order of $\lambda/\Delta\lambda$ = 10000 the instrument will be competitive with other grating monochromator concepts. The latter is not the case at the relatively large bending-magnet sources at Elettra.

4.3. Effect of aberrations and their removal

4.3.1. Arising along the length of the grating. In the classical orientation the most severe aberration for a plane grating in a divergent beam is the focus term. In this case, as described by Petersen (1982), the beam cross section will change in the dispersion plane of the grating, which will affect the beam divergence. This results in a variable virtual source position in this direction, which is found at a different distance than the real source. Consequently the diffracted beam has become 'astigmatic' and will need astigmatic optics for focusing into a stationary exit slit. This aberration will not be observed when the grating is operated in the off-plane orientation with the grating orientation for $\beta_1 = \alpha$. In this case the virtual and the real source distance remain identical. This facilitates the focusing which can be achieved with stigmatically focusing optics, in this case by use of an ellipsoidal mirror. It is now interesting that one can also reverse the beam trajectory in Fig. 4 without introducing additional aberrations. Then the beam would first be focused and the mirror/grating pair would thus be operated in a convergent beam.

Even though the focus aberration will not be found, some smaller aberrations will be introduced into the diffracted beam when the incident beam is either divergent or convergent. In order to provide the just discussed source-size-limited spectral resolution it is now important that the size of the virtual source does not increase in the dispersion direction, *i.e.* in the vertical direction z, compared with the real source size. The related aberration has already been discussed by Cash (1983), who derived it for a grating in conical diffraction to be used in a soft X-ray spectrograph. Here, coma arises from the fact that the grating, when used at grazing incidence, is no longer a 'thin' optical component but has become a 'thick' optics. In fact the beams which are diffracted for a given wavelength by a constant angle $\varphi_1 + \psi$ at the longitudinal limits of the beam footprint at the grating no longer perfectly overlap in the vertical direction after the diffraction. According to Cash (1983), the base width of the diffracted beam cross section grows by $\Delta A_z = (\varphi_1 + \psi)L'$, which can also be written as

$$\Delta A_z = \frac{\lambda}{p}\frac{A_x}{\theta}. \qquad (7)$$

When this beam cross section growth is now back-traced for a divergent incident beam to the original source distance, it will result in a growth of the virtual source size by the same

Table 2
Size of the virtual source ΔA_z according to equation (7) for different photon energies for a beam acceptance of A_x = 4 mm in the horizontal direction.

	E = 6 keV	E = 600 eV
For p = 820 nm	100 µm	140 µm
For p = 278 nm	300 µm	420 µm

amount. The effect of this aberration does not depend on any source property. Table 2 shows the related results for the growth of the virtual source size according to equation (7) as a function of photon energy and groove spacing. Compared with the related source sizes of s_z = 66 µm for Elettra bending-magnet sources and s_z = 20 µm for ESRF undulator sources, this blurring is found to be always excessively large. Consequently this coma aberration will have to be removed, as it will decrease the achievable spectral resolution. Cash (1983) removed this aberration in a convergent incident beam almost completely by employing a radial groove grating, in which all grooves converge to a point at the original focal distance. In the present configuration instead the coma aberrations can be removed when all grooves diverge from a point at the original source distance. In both configurations the achievable spectral resolving power remains source-size-limited; and as the gradient does not depend on the wavelength it will not restrict the tuning capabilities by use of such a grating in a monochromator. Now the need for the radial groove grating does not present a particular obstacle, as according to Koike & Namioka (2004) and McEntaffer *et al.* (2004) the required gradient in the groove density can be produced in holographically ruled ion-etched gratings.

4.3.2. Arising along the width of the grating. Another aberration arises from the finite width of the beam footprint at the grating. If one assumes the beam from a point source fills a rectangular or square aperture upstream of the grating, downstream of the grating the rays from a horizontal row in the entrance aperture will fall onto a slightly bent circle segment. When this segment is back-traced to the original source distance, this virtual source will be blurred, *i.e.* enlarged, vertically. The related source size increase can be predicted from equation (4).

One obtains

$$\Delta\vartheta = \frac{\partial}{\partial\psi'}\vartheta_1\Delta\psi' = \frac{1}{\vartheta_1}\frac{\lambda}{p}\Delta\psi'. \quad (8)$$

In the monochromator scheme in Fig. 4 one has $\Delta\psi' = A/D$ and by projecting the diffracted X-rays back to the position of the source the resulting source blur is

$$\Delta A_x = \Delta\vartheta D = \frac{\lambda}{p}\frac{A_z}{\vartheta_1}. \quad (9)$$

Instead, in the reversed orientation for $\Delta\psi' = A/F$ and by projecting the diffracted X-rays forward to the position of the focus at a distance F from the grating, the focus blur is

$$\Delta A_x = \Delta\vartheta F = \frac{\lambda}{p}\frac{A_z}{\vartheta_1}, \quad (10)$$

which is identical to equation (9)

As the monochromator is operated with $\vartheta_1 = \theta$ and with $A_x = A_z$, *i.e.* by employing a square entrance aperture, the blur according to (9) and (10) is identical to the blur calculated by use of equation (7), which is presented in Table 2. This blur occurs orthogonal to the previous one in the non-dispersing direction and will thus not affect the spectral resolution of the monochromator. However, it will lead to an increase of the focused monochromatic image in the exit slit beyond the source size limit for this direction. The source size limit can be achieved in this case only in a collimated beam, in which this aberration is absent. Instead, in a divergent/convergent beam the blur in the horizontal direction varies linearly with the beam size in the orthogonal vertical direction. For the indicated aperture and for a grating with 1220 lines mm^{-1} the blur is either smaller or of the order of magnitude of the related source sizes at Elettra and at ESRF, respectively. It could thus still be acceptable. Even the blur for the 3600 lines mm^{-1} grating, which is similar to the source size, could be acceptable at Elettra. Instead, for the operation at the ESRF the latter blur seems to be unacceptable, as it is significantly larger than the related source size. Obviously this will now lead to a significantly reduced photon density in the exit slit compared with the aberration-free solution in collimated light. On the other hand, when a grating is to provide a similar resolving power in the classical orientation, it will have a significantly smaller diffraction efficiency. Thus the photon densities in the exit slit will be rather similar in this comparison. Note that closure of the aperture in the appropriate direction in order to reduce the effects of this aberration will ultimately, and undesirably, decrease the achievable diffraction-limited spectral resolution.

5. Conditions for the installation of the proposed monochromator scheme

The described conical diffraction monochromator, when installed at synchrotron radiation sources, can cover the entire soft X-ray range up to hard X-rays with photon energies of the order of 8 keV with a single optical component. In any case it will require a horizontal beam deflection at the mirror/grating combination. Depending on the chosen or available beam-conditioning optics upstream of the monochromator either a radial groove grating or a grating with constant groove density needs to be employed in order to provide source-size-limited spectral resolution. As the manufacture of both is possible as holographically ruled ion-etched gratings, both can be considered equally. This offers several options for the monochromator installation or for its addition to existing monochromators. The present study concentrated primarily on the concept as shown in Fig. 4, which can be directly connected to the source in the presented or in the reversed orientation. In the vertical direction the optimum beam size can then be as small as the size of the focused monochromatic source image.

Table 3
Possibilities, drawbacks and required parameters for the installation of the described conical diffraction monochromator in previously described beamlines.

The required shapes of the mirrors are abbreviated. A single abbreviation refers to two-dimensionally focusing/collimating optics (par = paraboloidal mirror, ell = ellipsoidal mirror). A combination of two abbreviations refers to astigmatic optics in the vertical/horizontal direction. Any astigmatic combination with a plane mirror can be realised in a single cylindrical mirror, while the other combinations may require the use of a mirror pair.

Configuration in incident beam	Use constant groove grating	Use radial groove grating	Residual aberrations orthogonal to dispersion	Required refocusing optics	Comment	Note†
Two-dimensional collimation, par	×		No	Stigmatic par	Optimum	(1)
Divergent beam plane		×	Yes	Stigmatic ell	Proposed	(2)
Vertically collimated par/plane		×	No	Astigmatic par/ell		(3)
Horizontally collimated plane/par	×		Yes	Astigmatic ell/par		(4)
Vertically focused ell/plane		×	Yes	One-dimensional plane/ell		(5)
Horizontally focused plane/ell		×	Yes	One-dimensional ell/plane		
Two-dimensional focused ell		×	Yes	None	Fig. 4 reversed	(6)

† (1) The optimum solution can be realised by adding only the optics presented in Fig. 4 behind the collimation optics as discussed, for example, by Hunter *et al.* (1982). (2) This is the proposed concept presented in Fig. 4, which can be added as a new beamline. (3) Vertical beam collimation is quite common in X-ray beamlines; however, always combined with vertical beam deflection in the dispersing part of the optical concept. (4) Horizontal beam collimation is possible in the beamlines described by McNulty *et al.* (1996) and Paterson *et al.* (2011), which are operated as all horizontal deflection beamlines. This latter orientation will facilitate the installation of the system as shown in Fig. 4. (5) A related beamline is described, for example, by Cerino *et al.* (1980), which, however, is based on vertical beam deflection in the dispersing part of the optical concept. (6) This is the situation at the Nanoscopium beamline (Somogyi *et al.*, 2011), where the reversed configuration compared with the system in Fig. 4 could be realised easily as the optical concept is also here an all horizontal deflection configuration. In this case only the plane mirror/plane grating combination would have to be added.

In the orthogonal, now horizontal, direction the aberrations will increase the focused image size eventually to beyond the refocused source size, which will result in reduced flux density. This latter drawback can only be avoided when the incident beam is collimated at least in the vertical direction. However, such one-dimensional collimation will then be required to combine with an astigmatically refocusing optic, which may eventually require the refocusing to be decoupled into two independent mirrors. Installation behind a horizontally collimating mirror will permit the use of constant-spacing gratings. But again it will require an astigmatically refocusing optic; and it will not solve the problem of the horizontally increasing image size, as has already been found in the simplest setup. The use of focusing in one direction prior to the grating in either direction will allow only one-dimensional focusing to be used in the always orthogonal direction behind the grating. This is an advantage compared with the astigmatic refocusing. It requires a radial groove grating. However, it will not avoid the image growth in the horizontal direction. Consequently the optimum optical scheme is a slight modification of the originally proposed conical diffraction monochromator described by Werner & Visser (1981) for gratings with constant groove spacing. This will require one of the plane mirrors to be removed and the remaining components to be used in an all horizontal deflection scheme.

Table 3 now summarizes these findings and provides some comments regarding the installation in some previously reported schemes for X-ray monochromators.

As far as the driving scheme for the simultaneous rotation of the plane mirror and the plane grating is concerned, one recognizes that the tuning range for the angle of grazing incidence for the indicated limits in photon energy of 6 keV and of 600 eV is very limited with $0.55^\circ < \theta < 4^\circ$. For this limited angular range the variation of the lateral beam displacement in a mirror/grating combination can remain negligible compared with the source size in the horizontal direction even when the separation between the two components is not adjusted. For the presented reference monochromator properties it is required to keep the beam displacement at about twice the accepted beam size, *i.e.* to keep it at about 8 mm. In this case the translation of one of the components in the direction of the beam can also be avoided, and the length of both components can be limited to 400 mm. Then, for tuning, one will mostly apply only a single rotation of the mirror/grating pair, and occasionally the grating orientation angle α will be slightly readjusted. The driving schemes in the monochromators described by Jark & Kunz (1986) and by Jark *et al.* (2014) take into account similar mechanical simplifications.

6. Conclusion

A plane-grating monochromator, with only one grating in a simple driving scheme, can be used to tune the photon energy through the entire soft X-ray range ($E < 1$ keV) up to the hard X-rays ($E > 8$ keV) with rather high efficiency, when the grating is operated in the extreme off-plane orientation. As far as softer X-rays are concerned ($E < 1$ keV), the source-size-limited spectral resolution can be comparable with that provided by grating monochromators, which operate the grating in the classical orientation.

Acknowledgements

The author is grateful to Dr D. Eichert of Sincrotrone Trieste for helpful discussions.

References

Born, M. & Wolf, E. (1980). *Principles of Optics*, ch. 8.6. New York: Macmillan.
Cash, W. (1982). *Appl. Opt.* **21**, 710–717.
Cash, W. C. Jr (1983). *Appl. Opt.* **22**, 3971–3976.
Cerino, J., Stöhr, J., Hower, N. & Bachrach, R. Z. (1980). *Nucl. Instrum. Methods*, **172**, 227–236.
Chen, C. T. & Sette, F. (1989). *Rev. Sci. Instrum.* **60**, 1616–1621.

Cocco, D., Bianco, A., Kaulich, B., Schaefers, F., Mertin, M., Reichardt, G., Nelles, B. & Heidemann, K. F. (2007). *AIP Conf. Proc.* **879**, 497–500.
Compton, A. H. (1923). *Philos. Mag. Ser. 6*, **45**, 1121–1131.
CXRO (2015). *Mirror Reflectivity*, http://henke.lbl.gov/optical_constants/mirror2.html.
Dietrich, H. & Kunz, C. (1972). *Rev. Sci. Instrum.* **43**, 434–442.
ESRF (2015). *ESRF*, http://www.esrf.eu/Accelerators/Performance.
Frassetto, F., Cacho, C., Froud, C. A., Turcu, I. C. E., Villoresi, P., Bryan, W. A., Springate, E. & Poletto, L. (2011). *Opt. Express*, **19**, 19169–19181.
Greig, J. H. & Ferguson, W. F. C. (1950). *J. Opt. Soc. Am.* **40**, 504–505.
Hunter, W. R., Williams, R. T., Rife, J. C., Kirkland, J. P. & Kabler, M. N. (1982). *Nucl. Instrum. Methods Phys. Res.* **195**, 141–153.
Jark, W. (2012). *J. Synchrotron Rad.* **19**, 492–496.
Jark, W. (2013). *J. Synchrotron Rad.* **20**, 190–193.
Jark, W. & Eichert, D. (2015). *Opt. Express*, **23**, 22753–22764.
Jark, W. & Eichert, D. (2016). *J. Synchrotron Rad* **23**, 91–97.
Jark, W., Eichert, D., Luehl, L. & Gambitta, A. (2014). *Proc. SPIE*, **9207**, 92070G.
Jark, W. & Kunz, C. (1986). *Nucl. Instrum. Methods Phys. Res. A*, **246**, 320–326.
Koike, M. & Namioka, T. (2004). *AIP Conf. Proc.* **705**, 865–868.
Kunz, C., Haensel, R. & Sonntag, B. (1968). *J. Opt. Soc. Am.* **58**, 1415–1416.
Liu, T., Simon, R., Batchelor, D., Nazmov, V. & Hagelstein, M. (2012). *J. Synchrotron Rad.* **19**, 191–197.
Matsushita, T. (1983). *X-ray Monochromators*, in *Handbook on Synchrotron Radiation*, Vol. 1, edited by E. E. Koch. Amsterdam: North-Holland.
McEntaffer, R., DeRoo, C., Schultz, T., Gantner, B., Tutt, J., Holland, A., O'Dell, S., Gaskin, J., Kolodziejczak, J., Zhang, W. W., Chan, K.-W., Biskach, M., McClelland, R., Iazikov, D., Wang, X. & Koecher, L. (2013). *Exp. Astron.* **36**, 389–405.
McEntaffer, R. L., Osterman, S., Cash, W., Gilchrist, J., Flamand, J., Touzet, B., Bonnemason, F. & Brach, C. (2004). *Proc. SPIE*, **5168**, 492–498.
McNulty, I., Khounsary, A., Feng, Y. P., Qian, Y., Barraza, J., Benson, C. & Shu, D. (1996). *Rev. Sci. Instrum.* **67**, 3372.
Paterson, D., de Jonge, M. D., Howard, D. L., Lewis, W., McKinlay, J., Starritt, A., Kusel, M., Ryan, C. G., Kirkham, R., Moorhead, G., Siddons, D. P., McNulty, I., Eyberger, C. & Lai, B. (2011). *AIP Conf. Proc.* **1365**, 219–222.
Petersen, H. (1982). *Opt. Commun.* **40**, 402–406.
Schnopper, H. W., Van Speybroeck, L. P., Delvaille, J. P., Epstein, A., Källne, E., Bachrach, R. Z., Dijkstra, J. & Lantward, L. (1977). *Appl. Opt.* **16**, 1088–1091.
Somogyi, A., Kewish, C. M., Polack, F., Moreno, T., McNulty, I., Eyberger, C. & Lai, B. (2011). *AIP Conf. Proc.* **1365**, 57–60.
Takacs, P. Z., Qian, S.-N. & Colbert, J. (1987). *Proc. SPIE*, **0749**, 59–64.
Underwood, J. H. & Barbee, T. W. (1981). *Appl. Opt.* **20**, 3027–3034.
Werner, W. (1977). *Appl. Opt.* **16**, 2078–2080.
Werner, W. & Visser, H. (1981). *Appl. Opt.* **20**, 487–492.